Design of Energy Efficient Topologies for Wireless On-Body Channel

Wout Joseph[†], *member IEEE*, Bart Braem[‡], Elisabeth Reusens[†], Benoît Latré[†],
Luc Martens[†], *member IEEE*, Ingrid Moerman[†] *member IEEE*, and Chris Blondia[‡] *member IEEE*
[†] Ghent University / IBBT, Dept. of Information Technology
Gaston Crommenlaan 8 box 201, B-9050 Ghent, Belgium
Fax: +32 9 33 14899, E-mail: wout.joseph@intec.UGent.be
[‡] University of Antwerp / IBBT, Dept. of Mathematics and Computer Science
Middelheimlaan 1, B-2020, Antwerp, Belgium, E-mail: Bart.Braem@ua.ac.be

Abstract—**Advanced applications in the area of remote health monitoring can be realized by Wireless Body Area Networks (WBANs). This paper investigates the physical propagation channel at 2.45 GHz near real humans and presents an application for cross-layer design in order to optimize the energy consumption of single-hop and multi-hop network topologies. The characterization of the physical layer is an important element in the development of a WBAN. Propagation measurements are performed on real humans in a multipath environment and propagation models are proposed. As a cross-layer application, the proposed path loss models are used to evaluate the energy efficiency of different network topologies. The paper investigates which topology is the most energy efficient in WBANs: single-hop or multi-hop communication.**

I. INTRODUCTION

A Wireless Body Area Network (WBAN) offers many promising applications in health care, medicine, sports, and multimedia, all of which make advantage of the unconstrained freedom of movement a WBAN offers. A WBAN connects independent nodes that are situated in the clothes, on the body or under the skin of a person through a wireless communication channel. According to the implementation, these nodes are placed in a star or multi-hop topology [1]. A WBAN offers many promising, new applications in home/health care, medicine, sports, multimedia, and many other areas, all of which make advantage of the unconstrained freedom of movement a WBAN offers.

The wireless connection between the devices of a WBAN can occur at different frequencies. Often the ISM (Industrial, Scientific and Medical) frequency bands or UWB (Ultra Wideband) are used. The 2.4 GHz band here is selected because it is freely available and most practical existing technology for WBANs works in this band. This paper characterizes the physical layer for narrow band communication at 2.45 GHz between two half wavelength dipoles near humans. Measurements are performed in a multipath environment on real humans considering different parts of the human body. As an application, the propagation models of this paper are used to evaluate the energy consumption of single-hop and multi-hop topologies in wireless networks on the human body. The physical propagation analysis is used to investigate thoroughly the impact on the energy consumption on protocol level (cross-layer research) in order to determine the most optimal network topology in terms of energy efficiency.

Papers [2]–[10] characterize the wireless on-body channel for some specific configurations of the transmitter and receiver and provide physical-layer models. Moreover, [11]–[18] present important research concerning the on-body wireless propagation and antennas. [10], [19] indicate that multi-hop wireless networks are required and single-hop networks are very difficult to realize. In [20], [21] the physical-layer models are used for designing and testing energy efficient and reliable cross-layer protocols, i.e. combining the MAC (Medium Access Control) layer and network layer. The work of Zasowski [10] was a first attempt to justify the use of multi-hop in a WBAN, where intermediate hops are used for reaching the receiver. An energy model only applicable for UWB communication is used and it is concluded that the criteria whether to use a multi-hop strategy depend on the ratio of the energy consumption needed for decoding/coding and receiving/generating a UWB-pulse. In [22] reliability is experimentally investigated by measuring the packet delivery ratio without imposing a MAC-protocol. A multi-hop strategy turns out the most reliable.

The radios used in WBANs are very small, which leaves only limited space for a battery while recharging is not always possible. Furthermore, an important requirement for WBANs is a large lifetime of the network. Therefore, energy efficiency is of uttermost importance in order to increase the lifetime of the network and to meet the requirements.

Regular ad-hoc and sensor networks mostly use multi-hop communication where nodes in the network act as routers for other nodes to help guarantee connectivity. Implementations in a WBAN often assume single-hop communication where all information is sent directly to the receiver.

The outline of this paper is as follows. In Section II, the measurement setup and the investigated configurations are described. Section III discusses the the on-body path loss in a multipath environment using measurements on real persons. In Section IV, a network protocol is introduced and the proposed path loss models are used to examine the energy performance of single-hop and multi-hop network topologies. Finally, conclusions are presented in Section V.

II. CONFIGURATIONS AND MEASUREMENT SETUP

Two identical half-wavelength dipoles at 2.45 GHz [23], with a length of 5.7 cm and a diameter of 1 mm, are placed at various positions on the human body. The -10 dB bandwidth of $|S_{11}|$ is about 300 MHz at 2.45 GHz if placed at a distance of 5 mm from the body. The measurements are performed in a modern office. The dipoles are balanced for radiation near the human body using a $\lambda/4$-bazooka balun [24]. A vector network analyzer (Rohde & Schwarz ZVR) is used to determine the $S_{21}(f)$-parameter (with respect to 50 Ω) between transmitter Tx and receiver Rx antennas for the different positions. In all measurements the dipoles are placed parallel to each other and are lined up for maximal power transfer. The propagation channel characteristics depend strongly on the height of the antenna above the body [2]. In this paper we investigate the wireless channel for a separation of 5 mm between the body and the antennas. The wireless on-body channel for line-of-sight narrow band communication at 2.45 GHz along the arm, the back, the torso, and the leg is investigated. The various antenna positions on the body are shown in Fig. 1. The selection of the measurement points is made for typical WBAN sensor locations on different body parts.

In total 583 different antenna positions are investigated. The distance between the antennas varies from 5 cm up to 40 cm in steps of 1 cm. These measurements are performed on two persons: a man (height 1.73 m, weight 73 kg, BMI (body mass index) 24.4 kg/m^2) and a woman (height 1.69 m, weight 61 kg, BMI 21.4 kg/m^2), both 23 years old. 214 measurements along the stretched arm, 132 on the back, 102 on the torso, and 135 on the leg were performed, respectively.
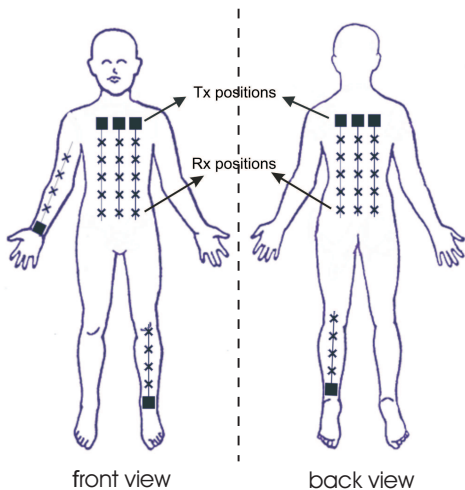

Fig. 1.   Antenna positions on the body (square = Tx and x = Rx).

III. PHYSICAL LAYER: PATH LOSS

A. Path loss model

To model the path loss between the transmitting and the receiving antenna as a function of the distance, we use the following semi-empirical formula [24]:

$$P_{dB}(d) = P_{0,dB} + 10n \, log(d/d_0) = -|S_{21}|_{dB} \qquad (1)$$

where the antenna separation d is expressed in cm, $P_{0,dB}$ is the path loss in dB at a reference distance d_0 (10 cm here), and n [-] is the path loss exponent, which equals 2 in free space. The path loss is defined as $-|S_{21}|_{dB}$ when the generator at Tx has an input impedance of 50 Ω and Rx is terminated with 50 Ω, which allows us to regard the setup as a two-port network for which we determine S_{21}.

Since the body is within the near field of the antenna, charges on both the antenna and body surfaces interact to create a single radiating system. In this case, it is no longer possible to separate the influence of the antenna from the influence of the body. Therefore, the antenna is included as a part of the channel model throughout this analysis [25]. The values and models that are determined in this measurement campaign are specific to our particular antenna, human bodies of the 2 persons, and office environment.

B. Measurement results

Fig. 2 shows the measured path loss versus Tx-Rx separation along the arm. The markers indicate the individual measurements, while the lines represent the path loss models obtained through fitting of the measurement data. Fig. 3 shows the fitted path loss models for all investigated body parts. Table I lists the parameter values of the fitted path loss models according to equation (1), and the variations of the measurement results around the model.
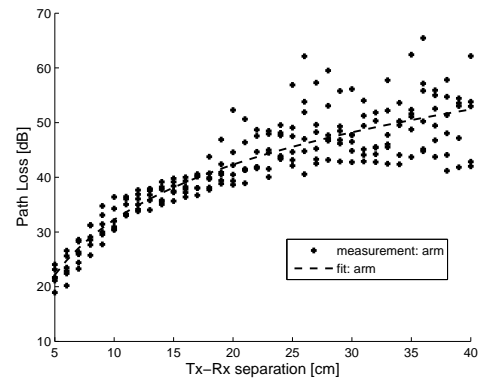

Fig. 2.   Measured path loss and fitted models versus antenna separation along the arm

The path loss increases with antenna separation as expected (Figs. 2 and 3. The path loss along the arm and the leg are very similar, see Table I and Fig. 3. The reference path loss and the path loss exponent of both models are almost the same: $P_{0,dB} \approx 32.4$ dB and $n \approx 3.4$. For the measured path loss along the leg, we observe a slightly higher variation around the path loss model (standard deviation $\sigma = 5.3$ dB) compared with the measurements along the arm ($\sigma = 4.1$ dB). This is because the measurements along the leg were performed on three different lines (front, side, and back), while along the arm only one line was investigated. The path loss model of (1) assumes that the coupling between Tx and Rx antenna is neglected for short seperations between the antennas. For a

seperation of down to 5 cm the coupling between the antennas close to the body is still acceptable as no clear deviation between model and measurements is observed in Fig. 2, 3.

The path loss along the torso follows the same course as the path loss along the arm, but the path loss along the torso is the highest of the investigated body parts. This is probably due to the higher absorption in the larger volume of the trunk, and because the surface of the trunk is less flat than the surfaces of the other investigated body parts. The path loss along the back follows a different course than the other three models. The path loss exponent is much lower ($n \approx 2.18$). This is because the surface of the back is more flat than the surface of the torso. The disparity in tissue compositions and in tissue thicknesses are another explanation for the variation between the path loss models for the different body parts. Due to different tissue compositions and thicknesses, the absorption in the specific body parts will vary, and thus the path loss along the body parts will differ.
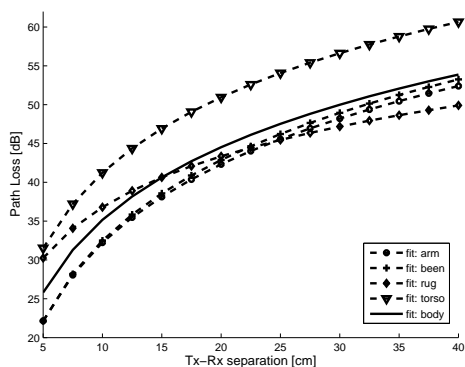

Fig. 3. Path loss models derived from measurements along the arm, torso, back and leg.

One can also define an average path loss model for the whole human body. For this purpose we consider a path loss model obtained through fitting of all measurement data. Fig. 3 shows the path loss models for the investigated body parts and for the measurements all together (full line). This curve lies between the previously derived path loss models. The parameter values of this model are also shown in Table I. The model is valid for line-of-sight communication, for the specified ranges 5 to 40 cm, and the investigated body parts (torso, back, arm, leg). Moreover the models are valid for the investigated subjects and the simulation model.

parameter	arm	leg	back	torso	body
$P_{0,dB}$ [dB]	32.2	32.5	36.8	41.2	35.2
n [-]	3.35	3.45	2.18	3.23	3.11
d_0 [cm]	10	10	10	10	10
σ [dB]	4.1	5.3	5.6	6.1	6.1

TABLE I
PARAMETERS OF THE DIFFERENT PATH LOSS MODELS.

C. Cumulative distribution function (CDF)

The model in equation (1) only represents the mean path loss [26]. In practice, there will be variations with respect to the nominal value. This variation is taken into account in the propagation model used in Section IV-B. It was shown in [27] that the variation around the mean path loss is well described by a lognormal distribution.

The mean values μ and the standard deviations σ of the lognormal distributions for the different body parts, fitted using a least-square error method, are provided in Table II. The values of these parameters indicate that the path loss models show very good correspondence with the measurement results. The mean values of the fitted CDFs of the deviation is close to 0 dB and the standard deviations differ less than 1 dB from the standard deviation of the measured values (Table II). Moreover, the different data sets also passed a Kolmogorov-Smirnov (K-S) test for normality at significance level 5 %, indicating that the deviation of measured path loss and model (in dB) is normally distributed [28].

	parameter	arm	leg	back	torso
PL_{dB}	σ [dB]	3.4	5.9	5.2	5.5
	μ [dB]	-0.2	-0.3	0.0	-0.7

TABLE II
PARAMETERS OF CDF OF DEVIATION BETWEEN MEASURED PL AND MODEL (LOGNORMAL DISTRIBUTION FIT).

IV. IMPACT ON ENERGY EFFICIENT NETWORK TOPOLOGY

In this section, we evaluate the energy consumption for narrowband communication at 2.4 GHz based on a commercial available radio. The goal is to investigate which topology is the most energy efficient in WBANs: single-hop or multi-hop communication. Firstly, a propagation model and an appropriate energy model are selected. Secondly, this energy model is subsequently used for analyzing the energy consumption.

A. Propagation model

When developing an energy model of the radio, it is important to distinguish between line of sight (LOS) propagation (in this paper) and non-line of sight (NLOS) situations (e.g., in [29] research about propagation around the torso for UWB-communication in a band of 3 to 6 GHz is performed). These models can be used for a narrowband system around 2.4 GHz as it is relatively close to the band of 3 GHz. Both models use (1), but with different parameters. For the LOS propagation, the parameters can be found in Table I (we use the whole body model). The NLOS propagation has the following parameter values: $d_0 = 10$ cm, $P_{0,dB} = 48.8$ dB, $n = 5.9$, and $\sigma = 5.0$ dB [29]. A higher path loss and a higher path loss exponent along the NLOS channel than along the LOS channel is observed due to diffraction around the human body and absorption of a large amount of radiation by the body.

The model in (1) only represents the mean path loss [26]. We also have to take the variations with respect to the nominal value into consideration. Therefore, a variation component (see

Section III-C) is included in propagation model. It is crucial to account for this, in order to provide a certain reliability of communications. The received signal strength $p_{r,dB}^j$ at a node j from a node i sending with transmitting power $p_{s,dB}^i$ over a distance $d_{i,j}$ between the nodes, can be written as

$$p_{r,dB}^j(d_{i,j}) = p_{s,dB}^i - P_{dB}(d_{i,j}) - X_{\sigma,dB} \quad [dBW] \quad (2)$$

where P_{dB} is the value predicted by the path loss model in equation (1) and the variation component $X_{\sigma,dB}$ is a zero-mean Gaussian random variable with standard deviation σ (specified by the path loss model). The condition for communication is that $p_{r,dB}^j$ is higher than a certain threshold p_{th} at the receiver. As a result, the probability $Con(i,j)$ that two nodes i and j are connected can be formulated as:

$$Con(i,j) = \Pr\left[p_{r,dB}^j(d_{i,j}) > p_{th}\right] \quad (3)$$

$$= \Pr\left[X_{\sigma,dB} - p_{s,dB}^i + P_{dB}(d_{i,j}) + p_{th} < 0\right] \quad (4)$$

$$= \frac{1}{2} - \frac{1}{2}\,\text{erf}\left(\frac{-p_{s,dB}^i + P_{dB}(d_{i,j}) + p_{th}}{\sqrt{2\pi}\sigma}\right) \quad (5)$$

If a reliable WBAN is desired, for example, a connection probability $Con(i,j)$ of 99% can be demanded.

B. Energy model

A good energy model of the radio is important for analyzing the energy efficiency of a network. Different energy models can be found in the literature. We have adapted the first-order model described in [30]. This model assumes a d^2 energy loss due to channel transmission with d the distance between Tx and Rx. Here, we transform the model in a more general one by changing d^2 to d^n, where n represents the path loss coefficient ($n = 3.11$ for the LOS channel and $n = 5.9$ for the NLOS channel). Doing so, the energy model becomes the following:

$$E_{tx}(k,d,n) = E_{TXelec} \cdot k + E_{amp}(n) \cdot k \cdot d^n \quad (6)$$

$$E_{rx}(k) = E_{RXelec} \cdot k \quad (7)$$

In these formulas, E_{tx} [J] represents the transmission energy, E_{rx} [J] the receiver energy, E_{TXelec} [nJ/bit] and E_{RXelec} [nJ/bit] the energy dissipated by the radio to run the circuitry for the transmitter and receiver respectively, $E_{amp}(n)$ [J/(bit·m^n)] the energy for the transmit amplifier, and k [bit] the number of bits sent. The radios are presumed to have power control and consume the minimal energy needed to reach the receiver. The specific values of these parameters are hardware dependent. We have determined these parameters for two commercially available transceivers which are frequently used in sensor networks: the Nordic nRF2401 low power single chip transceiver [31] and the Chipcon CC2420 transceiver [32] used in Telos-B motes. Both transceivers work in the 2.4–2.4835 GHz band and have a very low power consumption. The appropriate values for the parameters above were obtained by fitting equations (6) and (7) to the actual power consumption of the devices which can be found in the

datasheets. The distance used in equation (6) is the maximal distance that can be reached between Tx and Rx. If the receiver is positioned a little bit further, it is no longer within the receive range of the sender and the received signal is below the sensitivity of the radio. This maximal distance is calculated for each output power level (p_{tx}) using equations (1) and (2) and the assumption that the maximal path loss (P_{dB}) equals the difference between the sensitivity of the radio and p_{tx}. A reliability of 99% is assumed. Table III shows the results for both radios for the different values of the path loss exponent n for the LOS and the NLOS channel. It can be seen that the Nordic radio has a lower energy consumption per bit. This can be explained by the higher bitrate that can be obtained by the Nordic transceiver. Hence, we will use the parameters of the Nordic radios in our further calculations.

parameters	Nordic	Chipcon
E_{RXelec} [nJ/bit]	36.1	172.8
E_{TXelec} [nJ/bit]	16.7	96.9
$E_{amp}(n = 5.9)$ [J/(bit·m^n)]	7.99e-6	9.18e-4
$E_{amp}(n = 3.11)$ [J/(bit·m^n)]	1.97e-9	2.71e-7

TABLE III
PARAMETERS FOR ENERGY CONSUMPTION OF THE NORDIC NRF2401
AND CHIPCON CC2420 TRANSCEIVER.

C. Scenario

We want to show that a multi-hop approach is inevitable in a WBAN when evaluating the energy efficiency. Therefore, we consider a regular tree network as it allows a more generic way of approaching the problem. More specifically, we assume a ζ-balanced tree, i.e. a tree where all the children have exactly ζ children. In Fig. 4, a balanced tree with $\zeta = 2$ is depicted. There are L levels in the network that are numbered consecutively from level 1 for the nodes that are the furthest away from the sink up to level L for the nodes closest to the sink. We assume that the distance between the levels is fixed at an inter-node distance d_{in}. The spacing between the nodes is uniform in order to make the analysis more general. If a scenario was used with predetermined test locations of the nodes on the body, the results would only be applicable to that specific scenario. Indeed, it would be interesting to see how this scenario would behave, but this information can also be derived from our more general analysis with uniform spacing. As mentioned in Section IV-B, we distinguish between LOS and NLOS communication. The links between neighboring nodes is modeled as a LOS situation. In other situations, the path loss for NLOS is used. By using both LOS and NLOS, communication from one side of the body to the opposite is considered. Further, by changing the distance d_{in}, communication between a leg or arm can be modeled.

We assume that all nodes in the tree network generate packets at the same rate, so during each duty cycle each node wants to send one packet to the sink. Moreover, a perfect duty cycle is assumed, i.e. a sensor only turns on its radio when it sends or receives data. The main purpose of this approach is
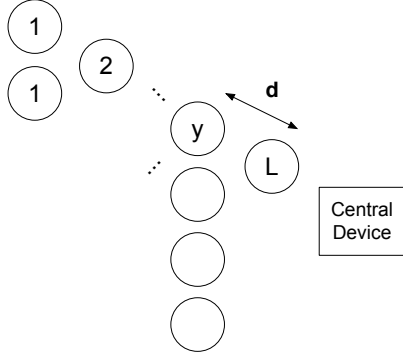
Fig. 4. Binary tree topology (ζ = 2) with fixed inter-node distance d_{in} and L levels.

to orthogonalize the results from this study and the properties of specific MAC-protocols.

As the energy efficiency is considered as one of the most important performance issues of WBANs, we use the network lifetime as metric, which we define as the time for the first node to die. In order to have a high network lifetime, the most consuming node should be made more energy efficient. This metric forces us to consider all nodes to be equally important, which corresponds to the fact that a WBAN has no redundant nodes.

We will try to improve the energy performance for this topology. In a first instance, we use a very simple type of multi-hop routing where the data is sent to the nearest neighbor. In a second instance, the multi-hop routing is made more complex by adding relay devices and by letting the nodes cooperate.

D. Single-hop versus multi-hop

In the tree network of Fig. 4, the energy usage per bit for a node at level y when using single-hop (E_{SH} [J/bit]) can be written as:

$$E_{SH}(y, d_{in}) = E_{TXelec} + E_{amp}(n)\left((L - y + 1) \cdot d_{in}\right)^n \quad (8)$$

Whereas the energy usage for a node at level y in a multi-hop network (E_{MH} [J/bit]) with the tree topology of Fig. 4 is given by:

$$E_{MH}(y, d_{in}) =$$
$$\zeta \cdot \sum_{i=0}^{y-2} \zeta^i \cdot E_{RXelec} \cdot k + \sum_{i=0}^{y-1} \zeta^i \cdot k \cdot \left(E_{TXelec} + E_{amp}(\eta) \cdot d_{in}^\eta\right)$$
$$(9)$$

Due to the ζ-balanced tree, each node has ζ children, what explains the factor ζ at the receiver part.

Fig. 5 shows the energy usage ratio E_{MH}/E_{SH} [-] of multi-hop versus single-hop scenario, in a tree network for $\zeta = 2$ with 4, 5 or 6 levels and d_{in} = 20 cm or 30 cm. If $E_{MH}/E_{SH} < 1$, then multi-hop is better and if $E_{MH}/E_{SH} > 1$, then single-hop is better.

The results show that the nodes closest to the sink (at level 6) perform really bad when using multi-hop: they become

hotspots using more than 100 times the energy of the single-hop scenario because they are relaying a lot of data from the nodes at the other levels. However, far away from the sink, at level 1 in Fig. 5, the single-hop scenario performs up to 1000 times worse than the multi-hop scenario because of the much higher path loss. It is clear that distance plays an important role in these results. When the distance between the nodes increases, the high path loss in the single-hop scenario has a dramatical impact on the performance, resulting in a higher energy usage.

E. Better energy efficiency by cooperation

The results obtained in the previous section are used to improve the energy efficiency of communication taking place in WBANs. The network lifetime can be improved by tackling the energy usage at the nodes consuming the most energy.

We observe that in the single-hop scenario, there is clearly room for energy saving at the nodes further away from the sink (see Fig. 5). These nodes consume the most energy and consequently will die first. However, we also see that in the multi-hop scenario more energy is consumed by the nodes closest to the sink (see Fig. 5), as they have to forward the data received from nodes further away. Based on these observations, we will consider the mechanism of cooperation (i.e., the nodes cooperate in forwarding the data from one node toward the central device) that can be used in order to improve the network lifetime.
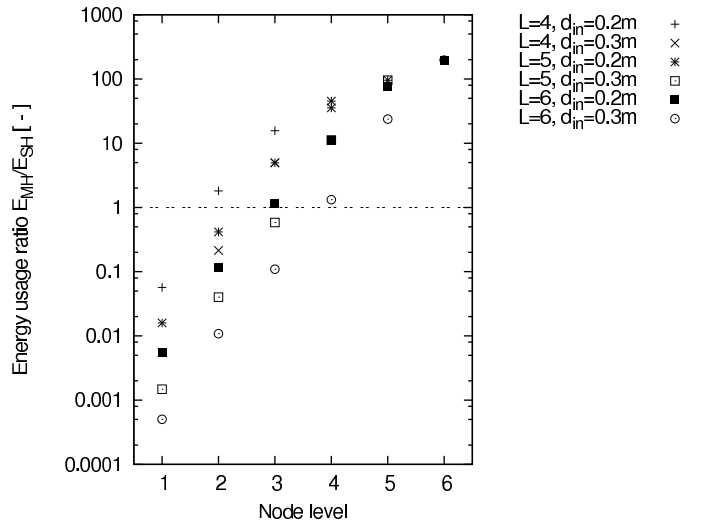

Fig. 5. Ratio of energy usage in the multi-hop scenario (E_{MH}) over energy usage in the single-hop scenario (E_{SH}) (tree topology (ζ = 2) with 4, 5 and 6 levels (L) and inter-node distance d_{in} = 20 cm or 30 cm).

When we compare the energy usage [J/bit] in a single-hop topology to the energy usage in a multi-hop topology in Fig. 6, it is obvious that there is a lot of residual energy available at higher levels, i.e. the nodes the closest to the central device. Indeed, by using this energy supply, the lifetime of the network will be bounded by the energy usage of the nodes on level 3. The data of the nodes on level 1 and 2 will be forwarded to level 4 and level 5, respectively. This will lower the energy

consumption of these nodes, as was the case with the relay devices. Hence, the network lifetime can be improved without the addition of extra relay devices.

The following formula is used to calculate the number of nodes that can be relayed by the nodes at level k when the energy consumption is limited by the nodes at level l:

$$\#\text{nodes supported} = \left\lfloor \frac{E_{SH}(l, d_{in}) - E_{SH}(k, d_{in})}{E_R(1, (L - k + 1) \cdot d_{in})} \right\rfloor \quad (10)$$

with $\lfloor \rfloor$ representing the floor function. Using this formula, it can be calculated that, e.g., for a network with an inter-node distance $d_{in} = 20$ cm, the data of up to 4 nodes can be relayed by the nodes at level 4.

Fig. 6 shows an example of the results when using the cooperation approach in a tree network with $\zeta = 2$ and $d_{in} = 20$ cm. The almost horizontal line of energy usage in the cooperating network demonstrates a good trade off between single-hop and multi-hop network setups, using a smart combination of both. We can also see that the energy consumption of a node at level 4 or 5 in the cooperating network (sending its own data and relaying the data of the other nodes) still remains slightly below the energy consumption of nodes at level 3. The maximal energy usage in the cooperating network (see Fig. 6) is a lot lower compared to the single-hop or multi-hop approaches, resulting in a higher network lifetime

These last results show that a smart combination of single and multi-hop networking will result in the most energy efficient network topology. This information can be used by protocol developers in order to create energy efficient routing protocols for WBANs. For example, this topology can be obtained by using a metric-driven protocol like [33] or by adaptation of other hop-based protocols such as [34].
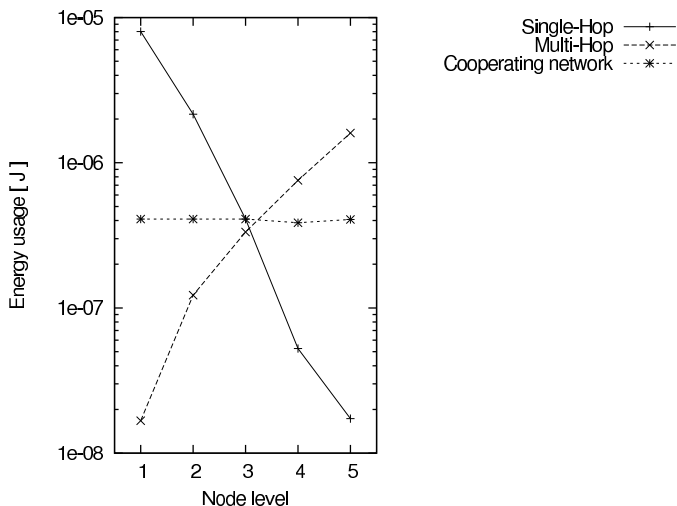

Fig. 6. Energy usage comparison between a single-hop, a multi-hop, and cooperating scenario (tree topology with $\zeta = 2$ and inter-node distance $d_{in} = 20$ cm).

V. CONCLUSIONS

Transmission between two half-wavelength dipoles near the human body is studied at 2.45 GHz. Propagation mea-surements are performed on real humans. The path loss is characterized for different parts of the human body. For the investigated subjects in a multipath environment, the path loss exponent is about 3.1 for line-of-sight communication. Path loss along arm and leg is similar. The path loss along the torso is the highest of the investigated body parts. The cumulative distribution functions of the deviation of measured path loss and models are well described by a lognormal distribution.

The propagation analysis is used to investigate an application on protocol level in order to determine the most optimal network topology in terms of energy efficiency. for the considered subjects, it is shown that single-hop communication is difficult in terms of energy consumption and multi-hop communication would be a better choice.

A more cooperative approach can improve energy consumption significantly, as this distributes the transmission load over the entire network. Based on the results carried out from this paper, metrics and algorithms should be developed that can decide which node to forward to and that allow a node to communicate whether it is capable of cooperating.

REFERENCES

[1] B. Latré, G. Vermeeren, I. Moerman, L. Martens, F. Louagie, S. Donnay, and P. Demeester, "Networking and propagation issues in body area networks," in *11th Symposium on Communications and Vehicular Technology in the Benelux*, Ghent, Belgium, Nov. 2004, available on CD-ROM.

[2] L. Roelens, W. Joseph, and L. Martens, "Characterization of the path loss near flat and layered biological tissue for narrowband wireless body area networks," in *International Workshop on Wearable and Implantable Body Sensor Networks (BSN 2006)*, MIT Media Lab, Boston, USA, Apr. 2006, pp. 50–53, available on CD-ROM.

[3] L. Roelens, S. Van den Bulcke, W. Joseph, G. Vermeeren, and L. Martens, "Path loss model for wireless narrowband communication above flat phantom," *IEE Electronics Letters*, vol. 42, no. 1, pp. 10–11, Jan. 2006.

[4] J. Ryckaert, P. De Doncker, R. Meys, A. de Le Hoye, and S. Donnay, "Channel model for wireless communication around human body," *IEE Electronics Letters*, vol. 40, no. 9, pp. 543–544, Apr. 2004.

[5] A. Alomainy, Y. Hao, X. Hu, C. Parini, and P. Hall, "UWB on-body radio propagation and system modelling for wireless body-centric networks," *IEE Proceedings-Communications*, vol. 153, no. 1, pp. 107–114, Feb. 2006.

[6] A. Fort, C. Desset, P. De Doncker, P. Wambacq, and L. Van Biesen, "An ultra-wideband body area propagation channel model - from statistics to implementation," *IEEE Trans. Microwave Theory and Tech.*, vol. 54, no. 4, pp. 1820–1826, Apr. 2006.

[7] E. Reusens, W. Joseph, G. Vermeeren, and L. Martens, "On-body measurements and characterization of wireless communication channel for arm and torso of human," in *International Workshop on Wearable and Implantable Body Sensor Networks (BSN 2007)*, Aachen, Germany, March 2007, pp. 264–269, available on CD-ROM.

[8] E. Reusens, W. Joseph, G. Vermeeren, D. Kurup, and L. Martens, "Real human body measurements, model, and simulations of 2.45 GHz wireless body area network communication channel," in *International Workshop on Wearable and Implantable Body Sensor Networks (BSN 2008)*, Hong Kong, China, June 2008, pp. 149–152, available on CD-ROM.

[9] E. Reusens, W. Joseph, B. Latre, B. Braem, G. Vermeeren, E. Tanghe, L. Martens, C. Blondia, and I. Moerman, "Characterization of on-body communication channel and energy efficient topology design for wireless body area networks," *IEEE Transactions on Information Technology in Biomedicine*, vol. 13, no. 6, pp. 933–945, Nov. 2009.

[10] T. Zasowski, F. Althaus, M. Stäger, A. Wittneben, and G. Tröster, "UWB for noninvasive wireless body area networks: channel measurements and results," in *2003 IEEE Conference on Ultra Wideband Systems and Technologies*, Reston, VA, Nov. 2003, pp. 285–289.

[11] P. Hall and Y. Hao, *Antennas and Radio Propagation for Body-Centric Wireless Communications*. London, UK: Artech House, 2006.

[12] P. S. Hall, Y. Hao, Y. I. Nechayev, A. Alomainy, C. C. Constantinou, C. Parini, M. R. Kamarudin, T. Z. Salim, D. T. M. Hee, R. Dubrovka, A. S. Owadally, W. Song, A. Serra, P. Nepa, and M. Gallo, "Antennas and propagation for for on-body communication systems," *IEEE Antenna and Propagation Magazine*, vol. 49, no. 3, pp. 41–58, June 2007.

[13] S. Kovacs, G. Pedersen, P. Eggers, and K. Olesen, "Ultra wideband radio propagation in body area network scenarios," in *ISSSTA Proceedings*, 2004, pp. 102–106.

[14] A. Alomainy, Y. Hao, A. Owadally, P. C., Y. Nechayev, P. Hall, and C. C. Constantinou, "Statistical analysis and performance evaluation for on-body radio propagation with microstrip patch antennas," *IEEE Transactions on Antennas and Propagation*, vol. 55, no. 1, pp. 245–248, January 2007.

[15] Y. Zhao, Y. Hao, A. Alomainy, and C. G. Parini, "Uwb on-body radio channel modelling using ray theory and sub-band fdtd method," *IEEE Transactions on Microwave Theory and Techniques, Special Issue on Ultra-Wideband*, vol. 54, no. 4, pp. 1827–1835, April 2006.

[16] S. L. Cotton and W. G. Scanlon, "Statistical analysis of indoor multipath fading fo a narrowband wireless body are network," in *IEEE 17th International Symposium on Personal, Indoor and Mobile Radio Communications*, September 2006, pp. 1–5.

[17] T. Tayamachi, Q. Wang, and J. Wang, "Transmission characteristic analysis for UWB body area communications," in *IEEE International Symposium on Electromagnetic Compatibility (EMC 2007)*, October 2007, pp. 75–78.

[18] A. F. Molisch, K. Balakrishnan, C. Chong, S. Emami, A. Fort, J. Karedal, J. Kunisch, H. Schantz, U. Schuster, and K. Siwiak, "IEEE 802.15.4a Channel Model - Final Report," IEEE 802.15.4a Channel Modeling Subgroup, Tech. Rep., 2004, online available at http://www.ieee802.org/15/pub/04/15-04-0662-02-004a-channel-model-final-report-r1.pdf.

[19] B. Braem, B. Latré, I. Moerman, C. Blondia, E. Reusens, W. Joseph, L. Martens, and P. Demeester, "The need for cooperation and relaying in short-range high path loss sensor networks," in *2007 International Conference on Sensor Technologies and Applications (SENSORCOMM 2007)*, Valencia, Spain, Oct. 2007, pp. 566–571.

[20] B. Latré, B. Braem, I. Moerman, C. Blondia, E. Reusens, W. Joseph, and P. Demeester, "A low-delay protocol for multihop wireless body area networks," in *Fourth Annual International Conference on Mobile and Ubiquitous Systems: Networking & Services (MobiQuitous 2007)*, Philadelphia, Pennsylvania, USA, Aug. 2007, pp. 1–8.

[21] B. Braem, B. Latré, C. Blondia, I. Moerman, and P. Demeester, "Improving reliability in multi-hop body sensor networks," in *The Second International Conference on Sensor Technologies and Applications (SENSORCOMM 2008)*, Cap Esterel, France, Aug. 2008.

[22] A. Natarajan, M. Motani, B. de Silva, K. Yap, and K. C. Chua, "Investigating network architectures for body sensor networks," in *HealthNet '07: Proceedings of the 1st ACM SIGMOBILE international workshop on Systems and networking support for healthcare and assisted living environments*. New York, NY, USA: ACM, 2007, pp. 19–24.

[23] L. Roelens, W. Joseph, E. Reusens, G. Vermeeren, and L. Martens, "Characterization of scattering parameters near a flat phantom for wireless body area networks," *IEEE Transactions on Electromagnetic Compatibility*, vol. 50, no. 1, pp. 185–193, Feb. 2008.

[24] C. A. Balanis, *Antenna Theory, Analysis and Design*. New York, NY: 1st ed. Harper & Row, 1982, pp. 64-65, 365-367.

[25] R. Vaughan and J. B. Andersen, *Channels, Propagation and Antennas for Mobile Communications*. Michael Faraday House, Stevenage, UK: Electromagnetic Waves Series 50, The Institute of Electrical Engineers (IEE), 2003.

[26] Saunders, *Antennas and propagation for wireless communication systems*. West Sussex, England: Wiley, 1999.

[27] A. Fort, C. Desset, J. Ryckaert, P. De Doncker, L. Van Biesen, and S. Donnay, "Ultra wide-band body area channel model," *IEEE International Conference on Communications (ICC)*, vol. 4, pp. 2840–2844, May 2005.

[28] M. H. Kutner, C. J. Nachtsheim, J. Neter, and W. Li, *Applied Linear Statistical Models, 5th ed.* Berkshire, UK: McGraw-Hill, 2005.

[29] A. Fort, J. Ryckaert, C. Desset, P. De Doncker, P. Wambacq, and L. Van Biesen, "Ultra-wideband channel model for communication around the human body," *IEEE Journal on Selected Areas in Communications*, vol. 24, pp. 927–933, Apr. 2006.

[30] W. Heinzelman, A. Chandrakasan, and H. Balakrishnan, "Energy-efficient communication protocol for wireless microsensor networks," in *Proceedings of the 33rd Annual Hawaii International Conference on System Sciences*, vol. 2, Jan. 2000, pp. 10 pp. vol.2–.

[31] "Nordic nrf 2401 datasheet." [Online]. Available: http://www.nordicsemi.no/index.cfm?obj=product&act=display&pro=64#

[32] "Chipcon cc2420 datasheet." [Online]. Available: www.chipcon.com/files/CC2420_Brochure.pdf

[33] T. Parker and K. Langendoen, "Guesswork: robust routing in an uncertain world," in *Mobile Adhoc and Sensor Systems Conference, 2005. IEEE International Conference on*, Nov. 2005.

[34] C. E. Perkins and E. M. Royer, "Ad-hoc on-demand distance vector routing," in *Mobile Computing Systems and Applications, 1999. Proceedings. WMCSA '99. Second IEEE Workshop on*, New Orleans, LA, USA, Feb. 1999, pp. 90–100.